Biosensors and Bioelectronics 86 (2016) 557–565

Contents lists available at ScienceDirect

Biosensors and Bioelectronics

journal homepage: www.elsevier.com/locate/bios

A sensitive and real-time assay of trypsin by using molecular imprinting-based capacitive biosensor

Gizem Ertürk [a,b], Martin Hedström [a,b], Bo Mattiasson [a,b,*]

[a] Department of Biotechnology, Lund University, Lund, Sweden
[b] CapSenze Biosystems AB, Lund, Sweden

ARTICLE INFO

Article history:
Received 8 June 2016
Received in revised form
11 July 2016
Accepted 12 July 2016
Available online 16 July 2016

Keywords:
Capacitive biosensor
Microcontact imprinting
Selectivity
Cross-reactivity

ABSTRACT

Use of a highly sensitive, selective capacitive biosensor is reported for label-free, real-time, easy and rapid detection of trypsin by using the microcontact imprinting method. Real-time trypsin detection was performed with trypsin-imprinted (trypsin-MIP) capacitive electrodes using standard trypsin solutions in the concentration range of 1.0×10^{-13}–1.0×10^{-7} M with a detection limit of 3.0×10^{-13} M. Selectivity and cross-reactivity of the system were tested by using competing proteins including chymotrypsin (chy), bovine serum albumin (BSA), lysozyme (lyz) and cytochrome c (cyt c) in singular and competitive manner and the selectivity of the system was determined with the selectivity coefficients of approximately 705.1, 6.5, 6.4 and 5.1 for chy, BSA, lyz and cyt c, respectively. The trypsin-MIP capacitive electrode was used for ~80 assays during 2 months and retained its binding property during all that time with a decrease of approximately 2.3% in the signal amplitude. In the last step, trypsin activity was measured by using N_{α}-Benzoyl-D, L-arginine 4-nitroanilide hydrochloride (BAPNA) as the substrate with spectrophotometer at 410 nm. The trypsin activity was measured as 9 mU/mL by spectrophotometer while the amount of captured enzyme calculated from the capacitive system was 7.9 mU/mL which shows the correlation between two methods. From the comparison it is obvious that the new method is an attractive alternative for assaying trypsin and the developed capacitive system might be used successfully to monitor label-free, real-time enzymatic activity of different proteases in a sensitive, rapid, cost-effective manner for different applications.

1. Introduction

Trypsin (EC.3.4.21.4) is a digestive enzyme produced by pancreas and responsible for the cleavage of proteins on the C-terminal side of arginine and lysine residues (Hirota et al., 2006). The determination of trypsin activity could be an indicator for diagnosis of pancreatitis, pancreatic cancer, cystic fibrosis, etc. which are related with alteration in pancreatic function (Artigas et al., 1981; Heinrich et al., 1979). While trypsin and trypsinogen levels increase with some types of pancreatic diseases including acute pancreatitis and cystic fibrosis, low or normal levels may be seen in chronic pancreatitis (Ionescu et al., 2006).

Traditional methods for the detection of trypsin or monitoring of trypsin activity mainly include gelatin degradation, spectrophotometric and sensitive radio-immunoassay based methods and also other methods based on Bragg reflector devices applications to measure the trypsin activity (Artigas et al., 1981; Kersey et al., 1993; Schwert and Takenaka, 1955; Spooncer et al., 1992; Temler and Felber 1976). Although several fluorometric assays of trypsin have been reported in recent years due to the advantages such as high sensitivity, easy operation and low background noise, all these techniques are time and cost consuming, require technical personnel and sophisticated laboratory equipment and many types of reagents including fluorophores (Gao et al., 2012; Hu et al., 2012; Li et al., 2013; Mu et al., 2010; Stoytcheva et al., 2012; Wang et al., 2010; Xue et al., 2010). Therefore, some biosensing devices are good alternatives to these methods with the advantages of allowing real-time, label-free, sensitive clinical analysis in a fast, precise and simple.

A colorimetric sensor was developed by Zhang and Du (2016) for detection of trypsin by using cytochrome c as the substrate and 3,3′,5,5′-tetramethyl benzidine (TMB)+hydrogen peroxide (H_2O_2) as the chromogenic agents. In the presence of trypsin, cyt c was hydrolyzed and released heme-peptide fragment, which exhibited an intensive catalytic role on H_2O_2-mediated TMB oxidization. The color of the solution changed into blue and the resultant color change could be monitored by the absorbance change at 652 nm.

* Corresponding author at: Department of Biotechnology, Lund University, Lund, Sweden.

http://dx.doi.org/10.1016/j.bios.2016.07.046
0956-5663/

Another technique reported by Dutta et al. (2016) is based on surface plasmon resonance (SPR) based detection of trypsin by using the camera of a smartphone. Zhang et al. (2014a) developed a turn-on chemiluminescent biosensor for label-free trypsin detection and screening of trypsin inhibitors using streptavidin modified magnetic beads. In another study, quantum dot based fluorescent assay has been developed for real-time monitoring activity of trypsin and of the trypsin inhibitor from soybean, Bowman-Birk type. The detection limit (LOD) was reported as 0.42 nM and the proposed method was simple and cost-effective (Zhang et al., 2014b).

Other alternative methods for trypsin detection are the electrochemical ones with the advantages including better detection limits and less complicated instrumentation. Zaccheo and Crooks (2011) reported a self-powered sensor for naked eye detection of trypsin with an assay time of ~3 h and a LOD value of 0.5 μg mL^{-1}. Another method which was developed by Stoytcheva et al. (2012) was based on electrochemical reduction of 1,2-benzoquinone on gelatin coated screen printed electrodes for square wave voltammetric determination of trypsin activity. Yi et al. (2014) reported an electrochemical immunosensor with multiwall carbon nanotubes (MWCNTs) composite modified electrodes for trypsin detection with a LOD value of 0.002 ng mL^{-1}. Although these developed sensors are sensitive, they have complicated construction, they require multi-step advanced processes including labeling and some of them are not suitable for real-time measurement.

The main objective of the present method was to develop a highly sensitive and selective biosensing system for label-free, real-time, easy and rapid detection of trypsin. For this purpose, capacitive biosensor was selected as the sensing platform. Capacitive biosensors are related to the sub-category of impedance biosensors (Berggren et al., 2001). The main advantages of capacitive biosensors are high sensitivity, real-time measurement, low power consumption, ease of detection, low-cost, flexibility in sensor size and volume reduction which make them attractive alternatives (Berggren et al., 2001; Berggren and Johansson, 1997; Ertürk et al., 2015; Hedström et al., 2005; Labib et al., 2010; Loyprasert et al., 2010; Mattiasson et al., 2010). We used microcontact imprinting method to prepare trypsin imprinted capacitive gold electrodes. The unique properties of microcontact MIPs (molecularly imprinted polymers), as introduced in previous reports (Chou et al., 2005; Ertürk et al., 2014; Ertürk and Mattiasson, 2016; Ertürk et al., 2016; Lin et al., 2006, 2007), make them attractive and promising for use as biomimetic sensor elements in biosensors. In the reported work, after determination of optimum conditions, trypsin detection was performed using the standard trypsin solutions. Selectivity and cross-reactivity of the system was indicated using proteins including chymotrypsin, bovine serum albumin (BSA), lysozyme and cytochrome c as the competing agents. In the last step the enzymatic activity of captured trypsin by the MIP-sensor, was determined by using BAPNA (N_{α}-Benzoyl-D,L-arginine 4-nitroanilide hydrochloride) as the substrate. Reusability of the system was demonstrated.

2. Materials and methods

2.1. Materials

Trypsin from bovine pancreas (cat. no. T-0134), tyramine (99%, $HOC_6H_4CH_2CH_2NH_2$), α-chymotrypsin from bovine pancreas (cat. no. C-4129), bovine serum albumin (cat no. A-3059), cytochrome c from horse heart (cat no. C-7752), N-isopropylacrylamide, N-hydroxymethylacrylamide, acrylamide, N,N′-Methylenebis(acrylamide), ammonium persulfate (APS), N,N,N′,N′-tetramethylethylenediamine (TEMED) and N_{α}-benzoyl-DL-arginine 4-nitroanilide hydrochloride were obtained from Sigma (Steinheim, Germany). Lysozyme from chicken egg white (cat no. 62971-10G-F), glutaraldehyde (50%, w/v), triethylamine, 3-aminopropyl-triethoxysilane (APTES) were purchased from Fluka (Buchs, Switzerland). Acryloyl chloride and 1-dodecanethiol were obtained from Aldrich (Deisenhofen, Germany).

Glass microscope cover slips (24 × 40 mm) (Menzel-Glaser) were used for the immobilization of template protein (trypsin). All other chemicals used were of analytical grade. All buffers were prepared with water treated with a reverse osmosis step with a Milli-Q system from Millipore (Bedford, MA, USA). Prior to use, all buffers were filtered through a Millipore filter (pore size; 0.22 μm) and degassed for 1 h.

2.2. Preparation of trypsin imprinted (trypsin-MIP) capacitive electrodes with microcontact imprinting method

Trypsin-MIP capacitive electrodes were prepared in three steps:

2.2.1. Preparation of glass cover slips (protein stamps)

Glass cover slips (24 × 40 mm) were modified and then used as protein stamps in the study. In the first step, they were cleaned as described before (Ertürk et al., 2014, 2015). Cleaned cover slips were immersed in 10% (v/v) APTES solution in ethanol at room temperature for 1 h to introduce amino groups on the surface of the cover slips. In the next step after proper washing in ethanol and distilled water, the modified cover slips were immersed in 5% (v/v) glutaraldehyde solution in 10 mM phosphate buffer (pH 7.4) at room temperature for 2 h to modify the amino groups on the surface as described in previous reports (Ertürk et al., 2014, 2015). Using an excess of glutaraldehyde resulted in that one of the aldehyde groups reacted with amino groups while the other was left unreacted. After proper washing, the cover slips were immersed in 0.1 mg mL^{-1} trypsin solution in phosphate buffer (10 mM, pH 7.4) at 4 °C, overnight for the immobilization of trypsin onto the activated surface. In the last step, after washing with phosphate buffer, water and drying with nitrogen gas, the cover slips were ready to be used as the protein stamp.

2.2.2. Preparation of capacitive gold electrodes

In the first step, gold electrodes were cleaned as described before (Ertürk et al., 2014). After plasma cleaning (Mod. PDC-3XG, Harrick, NY) for 30 min, electro-polymerization of tyramine was performed by cyclic voltammetry (CV) in ethanolic solution of 10 mM tyramine with a set potential range of 0–1.5 V (Ag/AgCl) and a scan rate of 50 mV s^{-1} for 15 scans to introduce free primary amino groups on the surface of the electrode via the deposition of poly-tyramine on the electrode, as described in previous reports (Erlandsson et al., 2014; Labib et al., 2010). In the next step, the electrodes were immersed in a solution containing 30 mM acryloyl chloride and 30 mM triethylamine (in toluene) overnight, at room temperature. Hence, the reaction of the acryloyl chloride with the free primary amino groups on the surface generated amide groups and left free vinyl groups that would be involved in the subsequent polymerization step. In the last step, the electrodes were rinsed with distilled water, phosphate buffer (10 mM, pH 7.4) and dried with nitrogen gas.

2.2.3. Microcontact imprinting of trypsin onto the modified capacitive electrode

A monomer solution containing hydroxymethylacrylamide, N-isopropylacrylamide (NIPAm), acrylamide, N,N-bisacrylamide in 10 mM phosphate buffer (pH 7.4) and TEMED (20 μL, 5%, v/v) was prepared and the initial monomeric mixture was degassed for

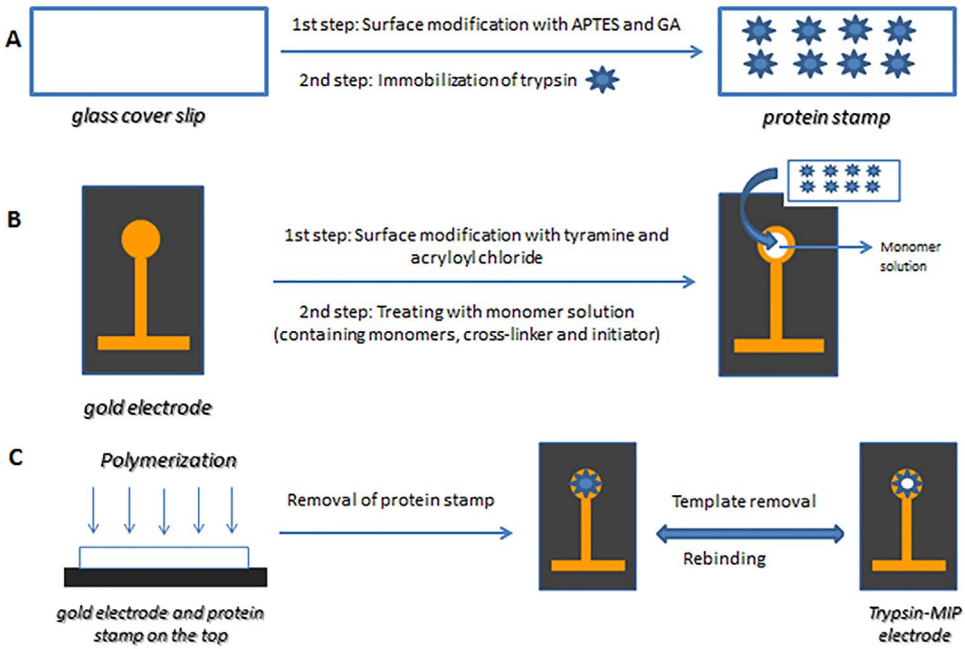

Scheme 1. Schematic representation of preparation of trypsin-MIP capacitive gold electrodes; (A) Preparation of glass cover slips (protein stamps), (B) Preparation of capacitive gold electrodes, (C) Imprinting of trypsin to the surface via microcontact imprinting method.

5 min. Fresh prepared initiator (APS) (20 μL, 10%, v/v) was added to this solution. Monomer solution (1.5 μL) was pipetted onto the modified gold electrode surface and the protein stamp (the glass cover slip) was brought into contact with the print molecules exposed to the monomer solution. The electrode was incubated for 3–5 h at room temperature. Then, the protein stamp was removed from the surface and the electrode was cleaned with 10 mM phosphate buffer (pH 7.4). Finally, the electrode was immersed in 1-dodecanethiol (10 mM in ethanol) for 20 min in order to cover pinholes in the insulating layer on the gold surface to ensure proper insulation. Ultimately the electrode was thoroughly washed with phosphate buffer (10 mM, pH 7.4). Schematic representation of the preparation of trypsin-MIP capacitive gold electrodes is shown in Scheme 1.

2.3. Surface characterization of trypsin-MIP electrodes

2.3.1. Cyclic voltammetry (CV) studies

CV experiments were carried out using a potentiostat/galvanostat (Autolab PGSTAT 12, EcoChemie, Utrecht, The Netherlands). Instrument operation and data acquisition were controlled using GPES 4.8 Software. All electrochemical measurements were conducted in a standard three electrode flow cell fitted with a platinum wire and a commercial Ag/AgCl electrode as the counter and the reference electrodes, respectively. Trypsin-MIP electrode was used as the working electrode. A solution of KCl (0.1 M) containing 0.1 M potassium ferricyanide was used as the electrolyte solution. CV was performed by sweeping the potential between −0.3 and 0.8 V at a sweep rate of 0.1 V s^{-1} as has been done in previous reports (Limbut et al., 2007; Loyprasert et al., 2010; Teeparuksapun et al., 2010). CV was used to evaluate the degree of insulation of the electrode surface after each step.

2.3.2. Atomic force microscopy (AFM) studies

In order to characterize the surface of bare gold electrodes and trypsin-MIP electrodes, atomic force microscope (AFM) (Veeco Instruments Inc, USA) in tapping mode was used. The electrodes were attached on a sample holder by using double-sided carbon strip. Scanning area (10 μm × 10 μm) and the vertical examination area (2.5 μm) were the experimental parameters.

2.3.3. Scanning electron microscopy (SEM) studies

Quanta 400F Field Emission SEM (USA) was used for scanning electron microscopy (SEM) analysis of the bare and trypsin-MIP capacitive electrodes with a resolution of 1.2 nm. Before observation, the bare and the trypsin-MIP electrodes were cleaned with water, dried with nitrogen gas and sputter coated with Au/Pd.

2.4. Real time trypsin detection with trypsin-MIP capacitive electrodes

2.4.1. Capacitive measurements

Capacitive measurements have been performed with an automated flow injection system (CapSenze Biosystems AB, Lund, Sweden). The trypsin-MIP electrode was inserted into the electrochemical flow cell which was connected to the continuous flow system. The capacitance measurement was performed based on the current pulse method as described by Erlandsson et al. (2014). The capacitance was calculated as a function of time from the resulting potential profile. The analyses were started with the injection of regeneration buffer (50 mM Glycine-HCl, pH: 2.5) into the system to regenerate the surface. This step was repeated between each analyte injection. After a stable baseline was recorded, standard solutions containing different concentrations of trypsin (1.0×10^{-13}–1.0×10^{-7} M) were injected sequentially into the system. The binding of trypsin (target) to the electrode surface resulted in a decrease of the registered capacitance owing to the displacement of the counter ions around the capacitive electrode that makes the change in the capacitance value. The change in capacitance (ΔC) was calculated automatically by CapSenze Smart Software (CSS) and there is a linear relationship between the logarithmic concentration of molecules bound to the surface of the electrode and the change in capacitance (ΔC). In all of the analyses, the flow rate was 100 μL min^{-1} and the injected sample volume was 250 μL.

The effects of type (phosphate or Tris-HCl, 10 mM) and pH (6.0–8.0) of the running buffer on trypsin detection were evaluated by monitoring the change in capacitance signal at the same

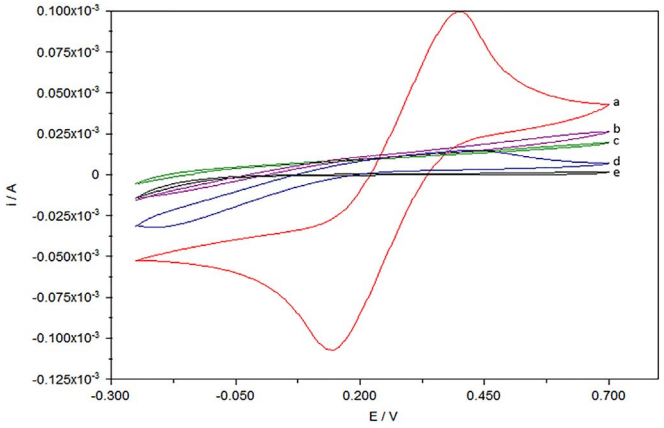

Fig. 1. Characterization of electrodes with cyclic voltammogram recorded in a solution of 100 mM KCl containing 100 mM $K_3[Fe(CN)_6]$ using: bare gold electrode (a-red), gold electrode after electro-polymerization of tyramine (b-purple), gold electrode after surface modification with acryloyl chloride (c-green), gold electrode after microcontact imprinting of trypsin (d-blue), gold electrode after treatment with 1-dodecanethiol (e-black). The scan range was from −0.3 V to 0.8 V (vs. Ag/AgCl) at a scan rate of 0.1 V s^{-1}. (For interpretation of the references to color in this figure legend, the reader is referred to the web version of this article.)

concentration of trypsin (10^{-7} M). Hence, optimum conditions were determined and the analyses were performed in these conditions in the following study.

2.4.2. Selectivity and cross-reactivity of trypsin-MIP capacitive electrodes

To determine the selectivity and specificity of trypsin-MIP capacitive electrodes against trypsin (try), chymotrypsin (chy), bovine serum albumin (BSA), lysozyme (lyz) and cytochrome c (cyt c) were used as the competing proteins. The response of the electrodes against these proteins was monitored while applying chy, BSA, lyz and cyt c solutions in singular manner and also mixed solutions including chy/try, BSA/try, lyz/try, cyt c/try and chy/BSA/lyz/cyt c/try in competitive manner to determine the cross-reactivity of the system.

Non-imprinted (NIP) capacitive electrodes were also prepared to show the imprinting selectivity of the trypsin-MIP electrode against NIP electrode. NIP electrode was prepared by the same method applied for trypsin-MIP electrode. However, during the preparation of the stamp for production of NIP, trypsin was not immobilized on the surface of the activated cover slips. The preparation and modification of the capacitive gold electrodes and the polymerization procedures were exactly the same for both trypsin-MIP and NIP electrodes. The response of NIP electrode to the competing proteins (chy, BSA, lyz, cyt c) was monitored.

2.4.3. Reusability of trypsin-MIP capacitive electrodes

Trypsin was detected repeatedly by using the assay cycle regeneration-equilibration-injection for 80 times. Reusability of the system was evaluated by monitoring the change in capacitance at the same concentration of standard trypsin solution (10^{-7} M).

2.4.4. Measurement of trypsin activity with trypsin-MIP capacitive electrodes

Trypsin is a pancreatic proteolytic enzyme which preferentially catalyzes the hydrolysis of peptide bonds between the carboxyl group of arginine and lysine and the amino group of another amino acid. N_α-Benzoyl-D,L-arginine 4-nitroanilide hydrochloride (BAPNA) is a chromogenic substrate for trypsin. Hydrolysis of BAPNA at the bond between the arginine and *p*-nitroaniline moieties releases the chromophore *p*-nitroaniline which can be detected by colorimetric analysis.

In the study, trypsin activity of the trypsin-MIP electrodes after exposure to a pulse of trypsin and subsequent proper washing was estimated by using BAPNA as the substrate. The procedure was as follows: 250 μL of a solution containing 1 mg mL^{-1} of trypsin was injected into the trypsin-MIP capacitive system. After washing with running buffer, the electrode with bound trypsin was taken out and incubated in 2.0 mL of substrate solution of BAPNA 0.5 mg mL^{-1} in Tris buffer (pH 7.8) at 37 °C for 30 min and the absorbance was read at 410 nm by the spectrophotometer at 5 min intervals. Tryptic activity was terminated with the addition of 2.0 mL 30% (v/v) acetic acid. One unit enzyme was defined as the amount of enzyme converting one micromole of BAPNA per minute at 25 °C and pH 8.1.

3. Results and discussion

3.1. Surface characterization of trypsin-MIP capacitive electrodes

Surface characterization of bare and trypsin-MIP capacitive electrodes was performed by using cyclic voltammetry (CV), atomic force microscopy (AFM) and scanning electron microscopy (SEM).

Proper insulation of the electrode surface is crucial in capacitive affinity based sensors as exemplified by immunosensors (Erlandsson et al., 2014; Loyprasert et al., 2010). The electro-polymerization of tyramine has been shown to produce insulating films carrying reactive amines on solid electrodes (Dai Tran et al., 2003). Insulating films formed with tyramine are rather thinner than the typical conducting polymer films and the electrodes material can be coated successfully without any damage in their electronic properties (Labib et al., 2010). Therefore, electro-polymerization of tyramine has been used as an insulation layer with the free primary amine groups, in the study. The degree of insulation can be probed by cyclic voltammetry of electro-active species in a contacting aqueous solution. The electrochemical characteristics of the prepared capacitive system were investigated by CV using the permeable redox couple $Fe(CN)_6^{4-/3-}$ after each fabrication step as shown in Fig. 1. The redox couple was oxidized and reduced during cycling of potential between – 0.3 and +0.8 V at a scan rate of 0.1 V s^{-1} at the clean gold surface according to the curves in Fig. 1. Electro-polymerization of tyramine brought about a consequent decrease in the redox peaks (Fig. 1, curve b), indicating a considerably reduced penetration of the conducting ions. The redox peaks decreased again after treating with acryloyl chloride in the next step as shown in Fig. 1 (curve c). After polymer formation, covalent binding of trypsin to the aldehyde groups on the surface of the electrode led to a further decrease in the redox peaks owing to the limited conductivity of proteins (Fig. 1, curve d). Finally, upon treatment with 1-dodecanethiol led to disappearance of the redox peaks and the lower current responses in both the anodic and cathodic processes that resulted in a highly blocked interface (Fig. 1, curve e). The long aliphatic chain of 1-dodecanethiol is employed to fill the defects in the formed layers to obtain a completely insulated electrode surfaces as reported in many of the previous reports (Gutierrez et al., 2015; Lebogang et al., 2014a, 2014b; Lenain et al., 2015). The electrochemical results indicate that the prepared electrode was highly insulated and could be further employed for detection.

AFM images of bare gold electrode and trypsin-MIP electrodes are shown in Fig. S.I. 1 (Suppl. Inf.). The surface morphology and surface deepness changed after polymer formation on the surface. A rough polymeric surface was formed on the surface of the electrode after polymerization.

Fig. 2A shows the surface morphology of the bare gold electrode and Fig. 2B–D show the surface morphology of trypsin-MIP

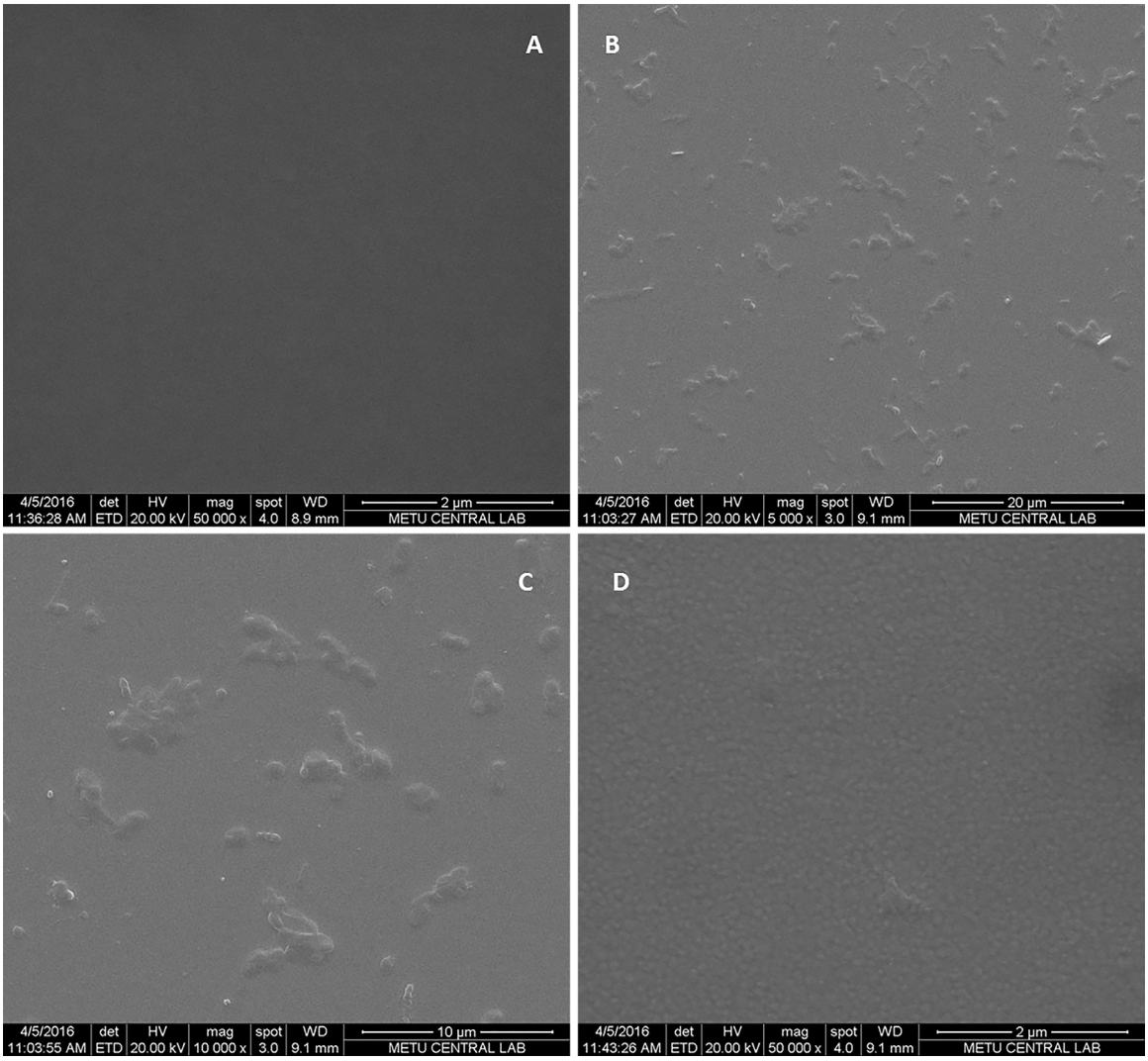

Fig. 2. SEM images of bare gold electrode (A-50,000 ×) and trypsin-MIP electrode in different magnifications (B-5000 ×), (C-10,000 ×), (D-50,000 ×).

electrode in different magnifications. The change in surface morphology of the bare gold electrode and trypsin-MIP electrode was shown in the SEM images. In Fig. 2B, C and D, the rough polymeric surface can be seen clearly when it is compared with the smooth surface in Fig. 2A. The results indicate that the polymeric film was successfully formed on the surface of the gold electrode via microcontact imprinting method. The size bars and the magnifications are shown on the figure.

3.2. Kinetic studies with trypsin-MIP capacitive electrodes

3.2.1. Optimization of the detection conditions

The trypsin-MIP capacitive electrode was inserted into the electrochemical flow cell which was connected to the automated flow injection system.

The operating conditions of the capacitive system were optimized for type and pH the running buffer. Prior to analysis, regeneration buffer (50 mM glycine-HCl, pH: 2.5) was injected into the system during 2.5 min to regenerate the system. In a previous report, glycine-HCl buffer was chosen for surface regeneration due to its good elution efficiency with only ~3% loss in the signal after 30 rounds of the binding-dissociation process (Huang et al., 2015). After waiting for 30 min for re-conditioning and re-equilibration of the system in running buffer, injection period started. Injection and equilibration period took in total 20 min. The capacitance graphs were obtained by plotting the change in capacitance ($\Delta C = -pF\,cm^{-2}$) versus the logarithm of trypsin concentrations. In order to obtain a reliable analytical signal, an average of five capacitance readings when the base-line had stabilized was calculated. For the influence of type and pH of running buffer on trypsin detection, 10 mM phosphate and 10 mM Tris-HCl were tested in the pH range of 6.0–8.0. Standard trypsin solutions (10^{-7} M) were prepared in each of these buffers and injected into the system. The highest change in capacitance was observed when 10 mM Tris-HCl in pH 7.4 was used as the running buffer as seen from Fig. 3A. However, the baseline was more stable, the capacitance change was more clear and reliable when 10 mM phosphate was used as the running buffer (pH 7.4) (Fig. 3A). In a previous study, optimum pH condition was determined using the quartz crystal microbalance (QCM) system and pH 7.5 was selected as the optimized pH since the change in frequency increased as the pH rose from 5.5 to 7.5 and then reached a plateau (Bayramoglu and Arica, 2012). In a previous QCM sensor study for trypsin detection, the optimum sensor effect was observed in pH 7.0 and a frequency shift of ~ 60% was obtained at pH 9.2 compared to pH 7.0, because the optimal pH of trypsin is in the range pH 8–9, auto-digestion of trypsin in solution might occur at this basic condition resulting in a gravimetric effect due to degradation of the enzyme (Hayden et al., 2006). Together with the results from the previous reports for trypsin detection and our results, it was decided to use 10 mM

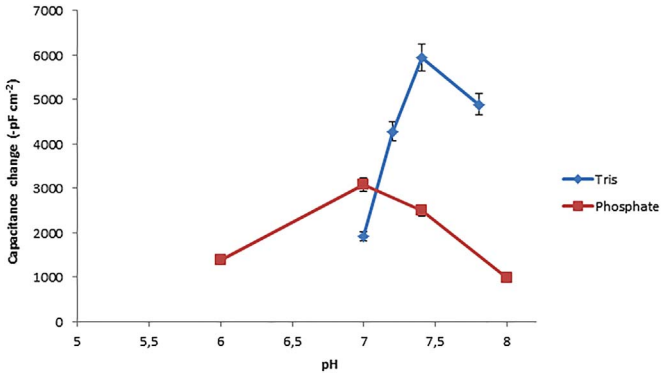

Fig. 3. Effect of type and pH of the running buffer on trypsin detection (trypsin concentration: 1.0×10^{-7} M; flow rate: 100 μL min^{-1}; sample volume: 250 μL; regeneration buffer: 50 mM glycine-HCl, pH 2.5; T 25 °C).

phosphate as the running buffer (pH 7.4) in the study.

3.2.2. Real time trypsin quantification with trypsin-MIP capacitive electrodes

After optimization of trypsin detection conditions, real-time trypsin detection studies from aqueous trypsin solutions were carried out with the trypsin-MIP capacitive system.

The running buffer was continuously pumped through the flow system at a flow rate of 100 μL min^{-1}. Trypsin solutions containing different concentrations of trypsin (1.0×10^{-13}–1.0×10^{-7} M) were prepared in the running buffer and sequentially injected into the capacitive system. Each solution was injected for 3 times. As seen from the actual sensorgram in Fig. 4B, the binding of trypsin to the electrode surface resulted in a decrease of the registered capacitance. CapSenze Smart Software automatically calculated the change in capacitance. The calibration graph that shows the capacitance change ($-$pF cm^{-2}) vs. log concentration of trypsin (M) is shown in Fig. 4A. The calibration graph was plotted from the logarithmic scale on the x-axis and a linear scale on the y-axis. As seen from the Fig. 4A, the ΔC value increased with the increasing trypsin concentrations. A linear relationship was obtained between the registered signal and the log concentration of trypsin in the concentration range 1.0×10^{-13}–1.0×10^{-7} M with the regression equation of y=354.11x+4705.2 ($R^2 = 0.972$). The limit of detection (LOD) was determined to be 3.0×10^{-13} M based on the IUPAC guidelines (McNaught and Wilkinson, 1997). LOD value was calculated based on the concentration derived from the smallest measure that is distinguished from the blank, which means the sum of blank value and three standard deviations of the blank.

A comparison of the LOD values for trypsin obtained from the present study and previous results (Arredondo et al., 2012; Chuang et al., 2016; Dutta et al., 2016; Hayden et al., 2006; Huang et al., 2015; Ionescu et al., 2006; Nemati et al., 2015; Schyrr et al., 2014; Stoytcheva et al., 2012; Wargocki et al., 2015; Yi et al., 2014; Zaccheo and Crooks, 2011; Zhang et al., 2014a; Zhang and Du 2016; Zhang et al., 2014b) is shown in Table 1. As seen from the table, the LOD value obtained from this study is comparable to those of the previous sensor studies for trypsin detection and it can be clearly seen that the value is one of the lowest.

3.2.3. Selectivity and cross-reactivity of trypsin-MIP capacitive electrodes

In order to test the selectivity of trypsin-MIP capacitive sensor for trypsin (try) (MW 23.3 kDa, pI 10.1–10.5), chymotrypsin (chy) (MW: 25.6 kDa, pI 8.3), bovine serum albumin (BSA) (MW: 66.5 kDa, pI 4.7), lysozyme (lyz) (MW 14.3 kDa, pI 11.35) and cytochrome c (cyt c) (MW: 12.3 kDa, pI 10.0–10.5) were selected as the competing proteins. Aqueous solutions of chy, BSA, lyz and cyt c were applied to the system in singular manner and also in competitive manner to determine the cross-reactivity. Standard protein solutions were prepared in the running buffer and the concentration of the proteins was 1 mg mL^{-1} and the molar concentrations of the proteins were 3.9×10^{-5} M for chy, 1.5×10^{-5} M for BSA, 7.0×10^{-5} M for lyz and 8.1×10^{-5} for cyt c while 4.3×10^{-5} M for try. As seen from Fig. 5A, the ΔC value was lower for all of the proteins compared to that of trypsin. The maximum ΔC value for the competing proteins was recorded after cyt c injection. Cytochrome c is a protein smaller than trypsin with a molecular weight of ~12.3 kDa and its isoelectric point is between 10.0 and 10.3, similar to that of trypsin. This could be the reason for the competitive effect of cytochrome c. The lowest selectivity coefficient was also recorded for cyt c as seen from Table 2. The concentrations of the interfering proteins and trypsin were 1.0 mg mL^{-1} in the selectivity experiments. If it is worked with the lower concentrations such as 1.0 μg mL^{-1}, then the selectivity of trypsin-MIP capacitive system over interfering proteins will be higher. It will not be possible to detect these interfering proteins in the lower concentration levels while it is possible for trypsin even in pg mL^{-1} concentration levels. Another important result is the very low affinity of the system towards chymotrypsin. Since chymotrypsin and trypsin are very similar proteins and found together in the pancreas, these results show the usability of the system for trypsin detection especially from pancreatic secretions.

As seen from the cross-reactivity results in Fig. 5B, pre-mixed solutions including the competitive proteins and trypsin caused a

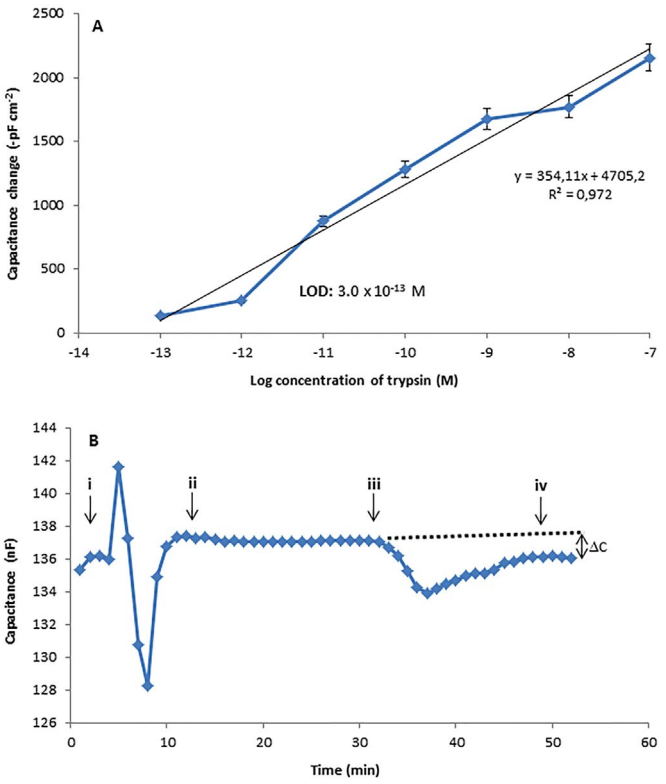

Fig. 4. (A) Capacitance change vs. logarithm of trypsin concentrations for trypsin-MIP electrode under optimum conditions (flow rate 100 μL min^{-1}; sample volume 250 μL; running buffer 10 mM phosphate, pH 7.4; regeneration buffer 50 mM glycine-HCl, pH 2.5; T 25 °C), (B) Actual sensorgram showing the capacitance change of trypsin-MIP electrode after injection of trypsin solution (1.0×10^{-11} M) under optimum conditions (i: before regeneration, ii: after regeneration, iii: before injection of trypsin solution, iv: after injection and re-equilibration with the running buffer) (flow rate 100 μL min^{-1}; sample volume 250 μL; running buffer 10 mM phosphate, pH 7.4; regeneration buffer 50 mM glycine-HCl, pH 2.5; T 25 °C).The dotted line is an extension of the stable baseline before injection, and ΔC is the change in signal registered upon injection of a trypsin containing sample.

Table 1
Comparison of analytical performances of different techniques used for trypsin detection.

Sensing principle	Sensor preparation method	Limit of detection (LOD)	Ref.
Colorimetric sensor	Employing cytochrome c as an enzyme substrate, 3,3′,5,5′-tetra-methylbenzidine as a chromogenic reagent	1.9×10^{-10} M	Zhang and Du, 2016
Liquid crystal (LC) sensor system	BSA immobilized gold grids as the enzymatic substrate	4.3×10^{-10} M	Schyrr et al. 2014
Interferometric sensor	Combination of chemically functionalized nanoporous anodic alumina photonic films and reflectometric interference spectroscopy	1.07×10^{-6} M	Arredondo et al. 2012
Localized SPR	Integration of light weight and simple laboratory optical components with the camera module of the smartphone	1.10×10^{-6} M	Dutta et al. 2016
Fluorescence detection system	Cell phone based portable bioassay platform	3.9×10^{-11} M	Reddy et al. 2012
Flow injection analysis-QCM biosensors	Immobilizing trypsin inhibitor as a specific ligand	0.16×10^{-6} M	Huang et al. 2015
Turn-on chemiluminescent biosensing platform	Using streptavidin-modified magnetic beads	1.0×10^{-11} M	Zhang et al. 2014a
Fluorescence based sensing	Functional high surface area scaffolds based on cellulose nanocrystals and polyvinyl alcohol	10.7×10^{-6} M	Osman et al. 2013
Electrochemical immunosensor	Multiwall carbon nanotubes (MWCNTs)-composite modified electrode	0.86×10^{-13} M	Yi et al. 2014
Fluorescent sensors	Quantum-dot based	0.42×10^{-9} M	Zhang et al. 2014b
QCM	Surface imprinting (molecular imprinting)	43×10^{-10} M	Hayden et al. 2006
Square wave voltammetric sensor	1,2-Benzoquinone electrochemical reduction on gelatin coated screen printed electrodes	4.3×10^{-10} M	Stoytcheva et al. 2012
Self-powered sensor	Signals the presence of trypsin via a light-emitting diode (LED) that is visible to the unaided eye	2.1×10^{-8} M	Zaccheao and Crooks 2011
Amperometric sensor	Two layer configuration; a polymer-glucose oxidase inner layer and a gelatin outer layer	42×10^{-12} M	Ionescu et al. 2006
Electrochemical method	Gelatin coated glassy carbon electrode	4.3×10^{-10} M	Tan and Wei, 2015
Capacitive biosensor	Microcontact imprinting of trypsin to the electrode	3.0×10^{-13} M	In this study

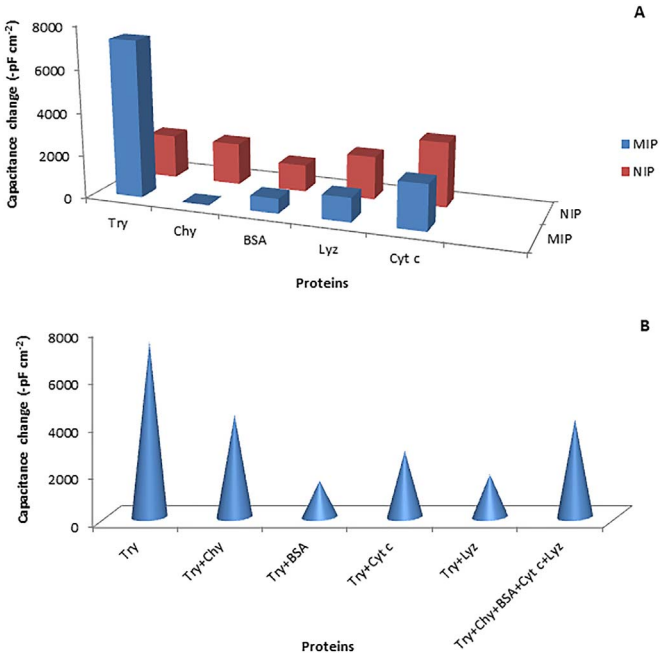

Fig. 5. (A) Selectivity of trypsin-MIP capacitive biosensor against competing proteins [chymotrypsin (chy), bovine serum albumin (BSA), lysozyme (lyz) and cytochrome c (cyt c)] in singular manner (protein concentration 1.0 mg mL^{-1}; flow rate 100 μL min^{-1}; sample volume 250 μL; running buffer 10 mM phosphate, pH 7.4; regeneration buffer 50 mM glycine-HCl, pH 2.5; T 25 °C), (B) Cross-reactivity of trypsin-MIP capacitive biosensor against competing proteins in pre-mixed solutions (protein concentration 1.0 mg mL^{-1}; flow rate 100 μL min^{-1}; sample volume 250 μL; running buffer 10 mM phosphate, pH 7.4; regeneration buffer 50 mM glycine-HCl, pH 2.5; T 25 °C).

lower capacitance response than could be stemmed from the competitive effects of the proteins over trypsin. However, it was observed that the trypsin-MIP system could detect trypsin in singular manner and also under competitive conditions. It is clear that the trypsin-MIP capacitive system enables the discrimination of trypsin even if it is coexisting with interfering proteins. In a previous colorimetric sensor study to evaluate the selectivity of

Table 2
Selectivity coefficients of trypsin-MIP and NIP electrodes [Δ: capacitance change for the trypsin-MIP and NIP electrodes, k: selectivity coefficient for trypsin versus competing proteins, k′: relative selectivity coefficient for trypsin-MIP electrode versus NIP electrode].

Protein	ΔC (pF) MIP	ΔC (pF) NIP	Selectivity coefficient (k) (MIP)	Selectivity coefficient (k) (NIP)	Relative selectivity coefficient (k′)
Trypsin	7331	2044	–	–	–
Chymotrypsin	10	1966	733.1	1.04	705.1
BSA	694	1266	10.56	1.61	6.54
Lysozyme	1128	2011	6.50	1.02	6.39
Cytochrome c	2118	3014	3.46	0.68	5.10

the assay for trypsin, six other proteins including lysozyme, thrombin, BSA, chymotrypsin, S1 nuclease and pepsin were used as the interfering proteins under the same experimental conditions. The absorbance (652 nm) was measured as 0.075 for lysozyme, thrombin, BSA and pepsin, 0.15 for S1 nuclease and 0.38 for chymotrypsin while it was 0.75 for trypsin (Zhang and Du, 2016). In a previous interferometric sensor developed for label-free, real-time quantification of trypsin, chymotrypsin and horse radish peroxidase (HRP) were selected as the competing proteins to test the chemical selectivity. While chymotrypsin molecules produced an almost negligible change (2.1 ± 0.5 nm) in the effective optical thickness, HRP produced a significant change (64.1 ± 2.5 nm) with a 2-fold lower value than produced by trypsin molecules (122.1 ± 5.2 nm). In another flow injection analysis-quartz crystal microbalance (FIA-QCM) biosensor developed for real-time dynamic analysis of protease inhibition in protein mixtures including BSA, ribonuclease A, cytochrome c, lysozyme and trypsin, the change in frequency was ~50 Hz while the change was ~70 Hz for trypsin in the individual injection assays (Huang et al., 2015).

The selectivity and cross-reactivity results of the present work indicate that the trypsin-MIP sensor's selectivity is comparable to the selectivity results obtained from previous sensors developed for trypsin detection.

The response of NIP sensor against competing proteins is also shown in Fig. 5A and the selectivity coefficients (k) are shown in

Table 2 and they were calculated as $\Delta C_{trypsin}/\Delta C_{competitor}$ and relative selectivity coefficient was calculated as k_{MIP}/k_{NIP}. As seen from the results, the trypsin-MIP sensor was more selective for trypsin than NIP sensor. In a previous report, imprinting capability of a family of acrylamide based MIPs for trypsin was characterized and the MIP/NIP selectivity ratios were calculated between 4:1 and 2:1 for different acrylamides (Reddy et al., 2012). In a QCM biosensor study developed with surface imprinting strategy for trypsin detection, the response for trypsin-MIP sensor was ~800 Hz while it was ~100 Hz for the NIP sensor (Hayden et al., 2006). As seen from the results in Table 2, relative selectivity coefficients show that the imprinted electrode could detect trypsin with a higher selectivity than what could be achieved with the NIP electrode. And the selectivity and relative selectivity coefficients obtained from our study show that the selectivity of the system is good and comparable to the previous results.

3.2.4. Reusability of trypsin-MIP capacitive electrodes

The trypsin-MIP capacitive system was also evaluated in terms of reusability by monitoring the change in capacitance ($-$pF cm^{-2}) at the same concentration of trypsin (10^{-7} M). The loss in the detection performance was approximately 2.3% after 80 analyses. The same trypsin-MIP capacitive electrode was used in whole experiment series and each of the analyses was repeated for 3 times. There was no significant change in the ΔC value after storage for 2 months at +4 °C. The results showed that the trypsin-MIP system could detect trypsin for a number of times without an obvious change in the efficiency. In a previous report, in order to test the reusability of the microcontact-myoglobin imprinted SPR sensor, 4 equilibration-adsorption-regeneration cycles were repeated (Osman et al., 2013). In another report, ~10 adsorption-desorption cycles were repeated by standard estradiol solution to show the reproducibility of 17-β estradiol imprinted film based biosensor (Tan and Wei, 2015). Altintas et al. (2015) reported that the nano-MIP based optical sensor they used in their study can be used at least for 12 months with ~30% decrease on Resonance Unit (RU) response. Atar et al. (2015) reported that triclosan imprinted SPR sensor has proved repeated mass shift during 5 equilibration-adsorption-regeneration cycles. Özkütük et al. (2013) reported that paraoxon-imprinted biopolymer based QCM sensor exhibited good reproducibility during 7 cycles with a loss of ~4% in the detection performance and proved its storage stability for more than 7 months with a slight loss of sensitivity. When compared to the previous reports, the reusability results obtained from our study is highly comparable and it shows that the microcontact imprinting technique has a significant advantage over others.

3.3. Measurement of trypsin activity with trypsin-MIP capacitive electrodes

In order to confirm the binding data obtained for trypsin by the capacitive sensor, experiments to quantify the captured enzyme by monitoring the enzymatic activity were performed. At 25 °C and pH 8.1, the enzyme activity of trypsin bound on the trypsin-MIP capacitive electrode was measured by a spectrophotometer at 410 nm. One unit of enzyme was defined as the amount of enzyme catalyzing the conversion of one micromole of substrate (BAPNA) per minute at 25 °C and pH 8.1. The trypsin activity was measured as 9 mU/mL by spectrohotometer (0.0090 μmol min^{-1}). The amount of captured enzyme calculated from the capacitive system was 7.9 mU/mL (0.0079 μmol min^{-1}). This result shows that there is a correlation between the amount of captured enzyme measured spectrophotometrically from the enzymatic activity and by the capacitive system. In the optimum reaction conditions (reaction time: 30 min, reaction volume: 1 mL, reaction temperature: 25 °C), all of the BAPNA is converted to the product (*p*-nitroaniline) in 30 min. When the trypsin-MIP electrode was regenerated with the regeneration buffer after binding of trypsin and then immersed in the substrate solution to check the trypsin activity, the activity was measured as 0.7 mU/mL by spectrophotometer (0.0007 μmol min^{-1}). This result shows that when the bound enzyme was removed from the surface by the regeneration step, the trypsin-MIP electrode did not have any enzymatic activity towards the substrate, as expected. Upon consideration of the advantages of the trypsin-MIP capacitive system in its real time, rapid determination, simplicity in operation and good sensitivity and selectivity, it appears to be an efficient technique for the assay of enzyme.

4. Conclusion

In the present study, by taking advantage of microcontact imprinting method and the capacitive biosensors, a simple, sensitive, selective, rapid, label-free and real-time detection system for trypsin has been developed. The results obtained from the sensing performance of the trypsin-MIP capacitive system revealed that the sensor presents a working range from 1.0×10^{-13} M to 1.0×10^{-7} M, a very low detection limit of 3.0×10^{-13} M, and a linearity of 97.2%. After injection of aqueous solutions of trypsin, it takes 20 min to find out the trypsin concentration. When the selectivity and cross-reactivity of the system were evaluated, the results revealed that the system is highly selective to the competing proteins with comparable selectivity values to what is described in previous reports. The developed sensing strategy could be used easily for the detection of other proteases and has a promising potential to be used as a point of care system for the development of efficient diagnostic kits toward some pancreatic diseases.

Acknowledgments

The authors are grateful to Dr. Dmitriy Berillo for valuable discussions.

This project was supported by The KK-Foundation for research, project number 20150086.

Appendix A. Supplementary material

Supplementary data associated with this article can be found in the online version at http://dx.doi.org/10.1016/j.bios.2016.07.046.

References

Altintas, Z., Guerreiro, A., Piletsky, S.A., Tothill, I.E., 2015. Sens. Actuators B – Chemical 213, 305–313.
Arredondo, M., Stoytcheva, M., Zlatev, R., Cosnier, S., 2012. ECS Electrochem. Lett. 1 (5), B1–B3.
Artigas, J., Garcia, M.E., Faure, M., Gimeno, A., 1981. Postgrad. Med. J. 57 (666), 219–222.
Atar, N., Eren, T., Yola, M.L., Wang, S., 2015. Sens. Actuators B – Chemical 216, 638–644.
Bayramoglu, G., Arica, M.Y., 2012. Bioprocess Biosyst. Eng. 35 (3), 423–431.
Berggren, C., Bjarnason, B., Johansson, G., 2001. Electroanalysis 13 (3), 173–180.
Berggren, C., Johansson, G., 1997. Anal. Chem. 69 (18), 3651–3657.
Chou, P.-C., Rick, J., Chou, T.-C., 2005. Anal. Chim. Acta 542 (1), 20–25.
Chuang, C.-H., Lin, Y.-C., Chen, W.-L., Chen, Y.-H., Chen, Y.-X., Chen, C.-M., Shiu, H.W., Chang, L.-Y., Chen, C.-H., Chen, C.-H., 2016. Biosens. Bioelectron. 78, 213–220.
Dai Tran, L., Piro, Bt, Pham, M.C., Ledoan, T., Angiari, C., Dao, L.H., Teston, F., 2003. Synth. Met. 139 (2), 251–262.
Dutta, S., Saikia, K., Nath, P., 2016. RSC Adv. 6 (26), 21871–21880.
Erlandsson, D., Teeparuksapun, K., Mattiasson, B., Hedström, M., 2014. Sens. Actuators B – Chemical 190, 295–304.

Ertürk, G., Berillo, D., Hedström, M., Mattiasson, B., 2014. Biotechnol. Rep. 3, 65–72.
Ertürk, G., Hedström, M., Tümer, M.A., Denizli, A., Mattiasson, B., 2015. Anal. Chim. Acta 891, 120–129.
Ertürk, G., Mattiasson, B., 2016. J. Chromatogr. B 1021, 30–44.
Ertürk, G., Özen, H., Tümer, M.A., Mattiasson, B., Denizli, A., 2016. Sens. Actuators B – Chemical 224, 823–832.
Gao, X., Tang, G., Li, Y., Su, X., 2012. Anal. Chim. Acta 743, 131–136.
Hayden, O., Haderspöck, C., Krassnig, S., Chen, X., Dickert, F.L., 2006. Analyst 131 (9), 1044–1050.
Hedström, M., Galaev, I.Y., Mattiasson, B., 2005. Biosens. Bioelectron. 21 (1), 41–48.
Gutierrez, A., Hedström, M., Mattiasson, B., 2015. Biotechnol. Rep. 8, 144–151.
Heinrich, H., Gabbe, E., Ičagić, F., 1979. Klin. Wochenschr. 57 (22), 1237–1238.
Hirota, M., Ohmuraya, M., Baba, H., 2006. J. Gastroenterol. 41 (9), 832–836.
Hu, L., Han, S., Parveen, S., Yuan, Y., Zhang, L., Xu, G., 2012. Biosens. Bioelectron. 32 (1), 297–299.
Huang, Y., Zhang, Q., Liu, G., Zhao, R., 2015. Chem. Commun. 51 (30), 6601–6604.
Ionescu, R.E., Cosnier, S., Marks, R.S., 2006. Anal. Chem. 78 (18), 6327–6331.
Kersey, A.D., Berkoff, T., Morey, W., 1993. Opt. Lett. 18 (16), 1370–1372.
Labib, M., Hedström, M., Amin, M., Mattiasson, B., 2010. Anal. Chim. Acta 659 (1), 194–200.
Lebogang, L., Hedström, M., Mattiasson, B., 2014a. Anal. Chim. Acta 826, 69–76.
Lebogang, L., Mattiasson, B., Hedström, M., 2014b. Microchim. Acta 181 (9–10), 1009–1017.
Lenain, P., De Saeger, S., Mattiasson, B., Hedström, M., 2015. Biosens. Bioelectron. 69, 34–39.
Li, X., Zhu, S., Xu, B., Ma, K., Zhang, J., Yang, B., Tian, W., 2013. Nanoscale 5 (17), 7776–7779.
Limbut, W., Hedström, M., Thavarungkul, P., Kanatharana, P., Mattiasson, B., 2007. Anal. Bioanal. Chem. 389 (2), 517–525.
Lin, H.-Y., Hsu, C.-Y., Thomas, J.L., Wang, S.-E., Chen, H.-C., Chou, T.-C., 2006. Biosens. Bioelectron. 22 (4), 534–543.
Lin, H.-Y., Rick, J., Chou, T.-C., 2007. Biosens. Bioelectron. 22 (12), 3293–3301.
Loyprasert, S., Hedström, M., Thavarungkul, P., Kanatharana, P., Mattiasson, B., 2010. Biosens. Bioelectron. 25 (8), 1977–1983.
Mattiasson, B., Teeparuksapun, K., Hedström, M., 2010. Trends Biotechnol. 28 (1), 20–27.
McNaught, A.D., Wilkinson, A., 1997. Compendium of Chemical Terminology. Blackwell Science, Oxford.
Mu, C.J., LaVan, D.A., Langer, R.S., Zetter, B.R., 2010. Acs Nano 4 (3), 1511–1520.
Nemati, M., Santos, A., Kumeria, T., Losic, D., 2015. Anal. Chem. 87 (17), 9016–9024.
Osman, B., Uzun, L., Beşirli, N., Denizli, A., 2013. Mater. Sci. Eng. C 33 (7), 3609–3614.
Özkütük, E.B., Diltemiz, S.E., Özalp, E., Gedikbey, T., Ersöz, A., 2013. Mater. Chem. Phys. 139 (1), 107–112.
Reddy, S.M., Phan, Q.T., El-Sharif, H., Govada, L., Stevenson, D., Chayen, N.E., 2012. Biomacromolecules 13 (12), 3959–3965.
Schwert, G.W., Takenaka, Y., 1955. Biochim. Biophys. Acta 16, 570–575.
Schyrr, B., Pasche, S., Voirin, G., Weder, C., Simon, Y.C., Foster, E.J., 2014. ACS Appl. Mater. Interfaces 6 (15), 12674–12683.
Spooncer, R., Al-Ramadhan, F., Jones, B., 1992. Int. J. Optoelectron. 7 (3), 449–452.
Stoytcheva, M., Zlatev, R., Cosnier, S., Arredondo, M., 2012. Electrochim. Acta 76, 43–47.
Tan, Y., Wei, T., 2015. Talanta 141, 279–287.
Teeparuksapun, K., Hedström, M., Wong, E.Y., Tang, S., Hewlett, I.K., Mattiasson, B., 2010. Anal. Chem. 82 (20), 8406–8411.
Temler, R.S., Felber, J.-P., 1976. Biochim. Biophys. Acta – Enzymology 445 (3), 720–728.
Wang, Y., Zhang, Y., Liu, B., 2010. Anal. Chem. 82 (20), 8604–8610.
Wargocki, P., Deng, W., Anwer, A.G., Goldys, E.M., 2015. Sensors 15 (5), 11653–11664.
Xue, W., Zhang, G., Zhang, D., Zhu, D., 2010. Org. Lett. 12 (10), 2274–2277.
Yi, Q., Liu, Q., Gao, F., Chen, Q., Wang, G., 2014. Sensors 14 (6), 10203–10212.
Zaccheo, B.A., Crooks, R.M., 2011. Anal. Chem. 83 (4), 1185–1188.
Zhang, H., Yu, D., Zhao, Y., Fan, A., 2014a. Biosens. Bioelectron. 61, 45–50.
Zhang, L., Du, J., 2016. Biosens. Bioelectron. 79, 347–352.
Zhang, W., Zhang, P., Zhang, S., Zhu, C., 2014b. Anal. Methods 6 (8), 2499–2505.